Title

Human Engineered Heart Muscles Engraft and Survive Long Term in a Rodent Myocardial Infarction Model.

Journal

Circulation research, 117(8)

ISSN

0009-7330

Authors

Riegler, Johannes
Tiburcy, Malte
Ebert, Antje
et al.

Publication Date

2015-09-01

DOI

10.1161/circresaha.115.306985

Peer reviewed

HHS Public Access

Author manuscript

Circ Res. Author manuscript; available in PMC 2016 September 25.

Published in final edited form as:

Circ Res. 2015 September 25; 117(8): 720–730. doi:10.1161/CIRCRESAHA.115.306985.

Human Engineered Heart Muscles Engraft and Survive Long-Term in a Rodent Myocardial Infarction Model

Johannes Riegler[1], **Malte Tiburcy**[4], **Antje Ebert**[1], **Evangeline Tzatzalos**[1], **Uwe Raaz**[1], **Oscar J. Abilez**[1], **Qi Shen**[1], **Nigel G. Kooreman**[1], **Evgenios Neofytou**[1], **Vincent C. Chen**[5], **Mouer Wang**[1], **Tim Meyer**[4], **Philip S. Tsao**[1,3], **Andrew J. Connolly**[2,6], **Larry A. Couture**[5], **Joseph D. Gold**[1], **Wolfram H. Zimmermann**[4], and **Joseph C. Wu**[1]

[1]Department of Medicine, Division of Cardiology and Stanford Cardiovascular Institute, Stanford University School of Medicine, Stanford, CA 94305, USA

[2]Department of Pathology, Stanford University School of Medicine, Stanford, CA 94305, USA

[3]Veterans Administration Palo Alto Health Care System, Palo Alto, CA

[4]Institute of Pharmacology, Heart Research Center, University Medical Center, Georg-August-University and German Center for Cardiovascular Research, Göttingen, Germany

[5]Center for Biomedicine and Genetics, Beckman Research Institute, City of Hope, Duarte, CA, USA

[6]Center for Applied Technology Development, Beckman Research Institute, City of Hope, Duarte, CA, USA

Abstract

Rational—Tissue engineering approaches may improve survival and functional benefits from human embryonic stem cell-derived cardiomyocte (ESC-CM) transplantation, thereby potentially preventing dilative remodelling and progression to heart failure.

Objective—Assessment of transport stability, long term survival, structural organisation, functional benefits, and teratoma risk of engineered heart muscle (EHM) in a chronic myocardial infarction (MI) model.

Methods and Results—We constructed EHMs from ESC-CMs and released them for transatlantic shipping following predefined quality control criteria. Two days of shipment did not lead to adverse effects on cell viability or contractile performance of EHMs (n=3, P=0.83, P=0.87). After ischemia/reperfusion (I/R) injury, EHMs were implanted onto immunocompromised rat hearts at 1 month to simulate chronic ischemia. Bioluminescence imaging (BLI) showed stable engraftment with no significant cell loss between week 2 and 12 (n=6, P=0.67), preserving up to 25% of the transplanted cells. Despite high engraftment rates and attenuated disease progression (change in ejection fraction for EHMs −6.7±1.4% vs control

Address correspondence to: Dr. Joseph C. Wu, 265 Campus Dr., Room G1120B, Stanford, CA 94305-5454, joewu@stanford.edu. Dr. Wolfram-H. Zimmermann, University Medical Center, 37075 Göttingen, Germany, w.zimmermann@med.uni-goettingen.de.

J.R. and M.T. contributed equally to this study.

DISCLOSURES

None.

−10.9±1.5%, n>12, P=0.05), we observed no difference between EHMs containing viable or non-viable human cardiomyocytes in this chronic xenotransplantation model (n>12, P=0.41). Grafted cardiomyocytes showed enhanced sarcomere alignment and increased connexin 43 expression at 220 days after transplantation. No teratomas or tumors were found in any of the animals (n=14) used for long-term monitoring.

Conclusions—EHM transplantation led to high engraftment rates, long term survival, and progressive maturation of human cardiomyocytes. However, cell engraftment was not correlated with functional improvements in this chronic MI model. Most importantly, the safety of this approach was demonstrated by the lack of tumor or teratoma formation.

Keywords

Human embryonic stem cells; myocardial infarction; cell survival; tissue engineering; engineered heart muscle; cardiac function; transplantation; cardiac magnetic resonance imaging; myocardial ischemia

INTRODUCTION

Myocardial infarction (MI) leads to a substantial loss of cardiomyocytes without significant endogenous regeneration in humans under the present state-of-the-art clinical practice[1]. Reduced force generation and increased stiffness of the infarct scar induce dilative remodelling which can ultimately result in heart failure and death[2]. The advent of efficient differentiation protocols that allow for the generation of billions of cardiomyocytes from pluripotent stem cells (PSCs), including both embryonic stem cells (ESCs) and induced pluripotent stem cells (iPSCs), has raised the prospect of cell therapies that aim to replenish lost cardiomyocytes with exogenously generated ones[3].

Preclinical and clinical studies on cell-based heart regeneration provide evidence that cardiac cell therapies may be realized via implantation of cell suspensions into or around the infarcted scar tissue[4–7]. Alternatively, tissue engineered heart muscle has been engrafted in allogeneic animal models with chronic and acute MI, providing evidence for enhanced cell retention and heart repair[8, 9]. Clinical translation of direct injection of autologous cell suspensions was relatively straight-forward, due to the adaptability of, for example, bone marrow stem cell processing procedures and availability of minimal invasive techniques for cell delivery. However, cell retention and survival are limited, typically preserving <5% of delivered cells at one month. Whereas, in acute or subacute cardiac disease, <5% might not be critical, especially if beneficial effects are primarily expected to be due to paracrine signalling. For chronic disease states with extensive ventricular scarring and with the goal to remuscularize the failing heart, however, cardiomyocyte retention is essential for maximum therapeutic impact and may be difficult to achieve by cell injections alone[10, 11].

Tissue-engineered constructs help to retain cells at the site of implantation and may, in addition, provide immediate mechanical support to the recipient heart. So far, a range of different cell types and biomaterials have been used to make such mechanical constructs (reviewed by Ye et al.[12]). *In vivo* studies have mostly been performed in rats, because of the availability of primary cardiomyocytes for allogeneic implantation of tissue engineered

grafts[8, 13, 14]. More recent studies have used fibrin or collagen hydrogels comprising human embryonic stem cell-derived cardiomyocytes (ESC-CMs) or scaffold free approaches[15–17]. Cell sheets made from ESC-derived cardiac progenitors have been tested in humans[18] and sheets made from induced pluripotent stem cell-derived cardiomyocytes (iPSC-CMs) have also been tested recently in preclinical models[19]. A challenge to the field is the construction of tissues of a critical thickness to provide mechanical assistance as well as a sustained transplant retention.

To address these challenges, we constructed macro-scale engineered heart muscle (EHM) from human ESC-CMs, by adapting a technique that has previously shown promising results with rat primary cells in a rat MI model[8]. We generated EHM loops using cell sources and a tissue engineering process compatible with good manufacturing practice (GMP). These loops were implanted onto chronically infarcted rat recipient hearts. Cell survival was tracked for up to 220 days using non-invasive imaging and histological characterization of graft size and composition. We quantified changes in infarct size, systolic function, and dilative remodelling using magnetic resonance imaging (MRI), as well as diastolic function using ultrasound. Finally, we demonstrated the feasibility of a decentralized EHM production and allocation facilitating clinical translation.

METHODS

An expanded Methods section is available in the Supplementary Materials.

Cultivation of human ESCs and differentiation to cardiomyocytes

Human H7 ESC line obtained from WiCell (Madison, WI) was expanded in a suspension culture system as previously described[20] to approximately passage 70. Cardiac differentiation was induced with small molecules CHIR99021 and IWP4. Cells were harvested at day 18 post induction. Cell viability, percentage of cardiac troponin T (cTnT), and CD90 positive cells were assessed using fluorescence activated cell sorting (FACS).

Generation of engineered heart muscle (EHM)

Human ESC-CMs (2.5×10^6) were first mixed carefully on ice with collagen type I and serum-free EHM medium and then cast into custom-made molds according to a previously published protocol[21]. Following condensation (5 days in casting molds), EHMs were transferred onto mechanical stretchers for functional maturation for an additional 12–14 days. EHM media was changed every other day. Following quality control (force of contraction > 0.1 mN/EHM loop measured by isometric force measurements), EHMs were shipped at room temperature with a temperature logger to record ambient temperature in 50 ml polypropylene tubes with 50 ml fresh media. Shipping conditions were established by testing EHM survival and function after 72 hr of mock shipments (EHM immersed in culture medium at an ambient temperature of 21°C). For the xenograft survival studies which relied on bioluminescence (BLI), EHMs were constructed from ESC-CMs expressing firefly luciferase and tdTomato red fluorescent protein (Fluc-tdT reporter line) using the above outlined procedure.

Force generation and viability of EHMs

Active force generation of EHMs was measured in organ baths prior to shipment in Göttingen, Germany and after receipt at Stanford in Tyrode's solution containing 1.8 mmol/L calcium under 1.5 Hz field stimulation for 1–4 EHM loops from each production lot[22]. Cell viability and cardiomyocyte content were assessed before and after shipping using TUNEL and cardiac troponin T staining.

Myocardial infarction (MI) and EHM transplantation

MI was induced in 8–10 week old male nude athymic rats (n=74, Charles River, Wilmington, MA) by occluding the left anterior descending (LAD) coronary artery for one hour. This was immediately followed by reperfusion. Surgery was performed aseptically under 1.5% to 2% inhaled isoflurane anesthesia. One month later, MRI and ultrasound imaging were performed, and rats were assigned to the different treatment groups (control n=14, EHM n=18, irradiated [not viable] EHM n=12, and long-term survival experiments n=14). Following baseline imaging (one month after MI), a second thoracotomy was performed and EHMs were attached to the left ventricular free wall using 8–12 stitches (7–0 Prolene). Rats received two EHM or stitches only for the control group. To evaluate a potential immune suppression regimen for EHMs following xenogeneic transplantation, immunocompetent male Sprague Dawley rats (n=7, Charles River) underwent the same procedure but received Tacrolimus (8 mg/kg/day; Astellas Pharma, Northbrook, IL) twice daily for 30 days. Rat surgeries were performed by an experienced microsurgeon (M.W.). For survival studies which relied on BLI, EHM made from (Fluc-tdT) reporter line CMs were implanted.

Bioluminescence imaging (BLI)

BLI was performed using the Xenogen *in vivo* Imaging System (Alameda, CA) as previously described[23]. See Supplemental Materials.

Magnetic resonance imaging (MRI)

Cardiac function and scar size were assessed one day before (i.e., one month after MI) and 28 days after EHM transplantation or sham surgery (control group) using a 7T MR901 Discovery horizontal bore scanner (Agilent Technologies, Santa Clara, CA) as previously described[24, 25].

Ultrasound imaging

On days when rats underwent MRI, pulsed wave Doppler and tissue Doppler US imaging were also performed to assess the diastolic relaxation of rat hearts using a Vevo 2100 ultrasound system (Visualsonics, Toronto, Canada). Diastolic dysfunction was defined as $E'/A' < 1$ following a previously published definition[26].

Immunohistochemistry and histological methods

Immunofluorescence and histological analyses were performed using standard protocols. See Supplementary Materials.

Statistical analysis

Results are shown as mean ± standard error mean (SEM). To test if there was a difference in cell viability, cardiomyocyte content, or force generation due to the transatlantic shipment, two-tailed Wilcoxon ranked sum tests were used. To test if a linear relation between number of viable cells and radiance as measured by BLI exists, we performed a regression analysis. To verify if the radiance from EHM patches or loops changed between day 14 and 85, a two-tailed Wilcoxon ranked sum test was used. To test if immune suppression in Sprague Dawley rats was a significant factor that might explain the observed variation in radiance and relative radiance, a linear mixed effects model with fixed effects for design, time, and random effects for individual rats was used (the residuals were tested for normality using a Shapiro-Wilk test). To test for differences in cardiac function, a linear mixed effects model was used with fixed effects for functional parameter, treatment group, time and a random effect for individual rats. If such an effect was found, the Wilcoxon ranked sum tests with Bonferroni corrections of p-values were then performed. For the comparisons of relative changes, the difference between day 28 and day −1 was calculated for each animal followed by one way ANOVA (residuals were tested for normality using a Shapiro-Wilk test). If such an effect was found, Wilcoxon ranked sum tests with Bonferroni corrections of p-values were then performed. Statistical analysis was performed using R software version 2.8.1.

RESULTS

Transatlantic shipment did not change cell viability or contractility of EHMs

To assess the feasibility of EHM generation and transplantation in a clinically relevant scenario, human ESCs were differentiated to cardiomyocytes (CMs) in spinner flasks at City of Hope following a GMP compatible protocol (Supplemental Figure IA). Production batches yielded up to two billion cells consisting of up to 95% CMs (Supplemental Figure IB,C). Cryopreserved cells were shipped from California to Germany. They were then thawed and cast into EHM loops, cultured for 17–19 days and shipped for two to three days from Göttingen, Germany to Stanford, California (Figure 1A–C). After arrival, EHMs were allowed to recover for one day in an incubator followed by force measurements and histological examinations. Shipment did not lead to adverse changes in cell viability (n=3, P=0.83), viable CM content (n=3, P=0.86), or active force generation (n=3, P=0.87, Figure 1D; Supplemental Figure ID–I), highlighting the feasibility of decentralized production and shipment to application sites. EHM exhibited an average force of 0.35±0.11 mN per EHM loop (n=9) which is equivalent to 1.07±0.84 nN/viable EHM-CM. Differences in CM yield of two differentiation batches used to make EHMs led to slight differences in contractile force and viable CM content prior to their implantation (Supplemental Figure II).

Interestingly, when we performed TUNEL staining, we noticed that human nuclear antigen antibody (hNA) labelled only TUNEL negative cells, indicating the potential suitability of hNA positive cells as surrogates for viable human cells (Supplemental Figure IIIA–D). Closer examination of EHMs revealed regions of densely packed cardiomyocytes with aligned sarcomeres reminiscent of embryonic cardiac tissue typically on the outer edges of EHM (Figure 1E). The majority of EHM cross-sections exhibited cardiomyocytes aligned along the primary strain axis, clustered together in band-like structures (Figure 1F,G).

Cardiomyocytes in these bands showed organized sarcomeres but exhibited little connexin 43 expression, highlighting these cells' immature phenotype.

EHMs demonstrated stable engraftment after week two following implantation

In order to assess long-term survival, EHM were made with CMs from a firefly luciferase and tdTomato (Fluc-tdT) reporter line. Differentiation of reporter line ESCs to CMs using a monolayer version of the small molecule protocol yielded between 80–90% CM purity (Supplemental Figure IVA,B). EHMs made from these cells generated a strong bioluminescent signal before and after transplantation onto infarcted hearts of nude rats (Figure 2A). The BLI signal of implanted grafts declined for the first two weeks following implantation. However, no significant decline was found between week 2 and week 12 (n=6, P=0.33), indicating stable long-term engraftment and survival of up to 25% in individual rats with an average of 10±4% (Figure 2B,C). We used relative radiance (radiance normalized to an initial maximum) as a surrogate for cell viability and engraftment since we observed a strong linear correlation between viable cells and measured average radiance (Supplemental Figure IVC–E, intercept: P=0.30, slope: P=2.2E-16).

EHM graft survival in immunocompetent rats with immune suppression is comparable to nude rats. Further development of EHMs as a potential therapy for heart failure will require functional assessments in larger animal models for which no immunocompromised strains exist to date. Thus, we also decided to test the suitability of Tacrolimus to prevent EHM rejection in immunocompetent Sprague Dawley (SD) rats. As expected, transplantation of EHMs without immune suppression led to rejection and almost complete cell loss after one week (n=2). In contrast, twice daily oral administration of Tacrolimus enabled cell survival similar to implantations in nude rats illustrating the suitability of this approach (Figure 2D,E, n=5, SD+Tacrolimus, n=6 nude rats; P=0.88).

EHM grafts consist primarily of cardiomyocytes one month after implantation

Human EHMs could be delineated on H&E or Masson's trichrome stained section via a small layer of fibrotic tissue separating them from the host myocardium (Figure 3A–D). Although EHMs contained a substantial number of cell debris, and CMs were primarily aligned in band-like structures, one month after implantation, we observed human grafts consisted of densely packed CMs. We did not observe any fibroblasts in these grafts regardless of the fibroblast content in cell batches used to make EHM. Human grafts were found in all analysed animals that received EHM (5/5 rats; Figure 3E,F). Cells staining positive for human markers were almost exclusively CMs interspersed with host derived vessels (Figure 3E). Cardiomyocytes themselves were not aligned along the major strain axis and they expressed little connexin 43 (Figure 3F). In line with this early embryonic phenotype, sarcomere width was small, not spanning the width of cells (Figure 3G).

EHM grafts contained few rat macrophages dispersed in the graft, indicating stable engraftment, corroborating our BLI data (Figure 3H). Graft thickness was typically 300–400 μm leading to a graft size of 0.5±0.1 mm^3 (n=5) at one month after implantation (Supplemental Figure VA,B). Only a small number of human nuclei were in an active state of the cell cycle as evidenced by Ki67 labelling (0.95±0.15%, Supplemental Figure VC,D).

High cardiomyocyte engraftment rates did not translate into significant functional improvements

It is unlikely that a cardiac patch or cardiomyocyte cell suspensions could be implanted shortly after MI in humans since this would require manufacturing immune matched patches or cells in advance and might interfere with other acute treatment strategies. Hence we focused on whether EHM implantations would have any effects on the recipient hearts in a chronic MI model. For that, implantation of EHM (n=14), irradiated EHM (n=9, a control for mechanical effects and dead cells), or control surgery (n=12, sham) was performed one month after MI. Systolic function and scar size (assessed by MRI) as well as diastolic relaxation (assessed by ultrasound) were measured one day prior to and one month after implantation or sham surgery (Figure 4A–C, Supplemental Figure VI). End-diastolic and end-systolic volumes increased over time in all groups (Figure 4D,E). While increases in end-diastolic volumes were not significantly different (P=0.35), end-systolic volumes increased faster in the control group compared against EHM group (control n=12 vs. EHM n=14; P=0.04). This difference was also reflected in a more pronounced decline in ejection fraction for the control group compared to EHM and irradiated EHM groups (P=0.03, Figure 4F–G). Notably, changes in ejection fraction were not different between viable and non-viable (lethally irradiated) EHM (P=0.19). This finding is consistent with the anticipated lack of electrical integration of human xenografts in rat hearts, but highlights the possibility that cell independent effects (e.g., activation of immune cells, mechanical stabilization) could also elicit therapeutic effects. EHM implantations did not lead to any changes in scar size either (P=0.32, Figure 4H–J). Finally, we reasoned that EHM transplantation may impact diastolic function because of left ventricular stiffening. We did not observe any significant changes in diastolic function due to EHM transplantations (control treatment n=9, EHM n=12, irradiated EHM n=8; P=0.12, Figure 4K). Morphologically, irradiated EHMs did contain high numbers of fibroblasts/myofibroblasts and macrophages (Supplemental Figure VII). A summary of all parameters measured via MRI and ultrasound can be found in Supplemental Tables I, II and Supplemental Figure VIII.

Long-term engraftment led to more mature cardiomyocyte organization

Tumor or teratoma formation is the primary safety concern for all cell therapies derived from pluripotent cells. In addition, regenerative therapies need to demonstrate functional integration of transplanted cells into the host tissues. To address these concerns, EHMs were analyzed at 110 (Figure 5A–D) and 220 days (Figure 5E–H) after implantation. No tumors or teratomas were found in any of these rats at 110 or 220 days (n=9 and n=5, respectively). Human grafts contained a high number of host derived blood vessels, almost comparable to normal myocardium (Figure 5A,E, Supplemental Figure IXA,B). Cardiomyocyte alignment as well as connexin 43 expression increased from day 110 to day 220 reaching a level similar to later fetal development stages in humans (Figure 5B,F). Cardiomyocytes exhibited well organized sarcomeres which frequently spanned the width of cells and aligned with the circumferential strain axis (Figure 5C,G). Grafts contained a small number of human cells which were in an active state of the cell cycle (0.93±0.18%, Figure 5D,H). While long-term engraftment induced CM maturation, we also found occasional areas in grafts consisting of clusters of glycogen-rich cells exhibiting a hamartoma-like phenotype (n=4 out of 4 rats tested), characterised by large “spider” cells containing cleared areas and intervening strands

of cytoplasm (Figure 5I). Fewer and smaller cleared cytoplasmic areas were found at day 110 compared to day 220, but cells were rich in glycogen, indicated by Periodic acid-Schiff staining (Supplemental Figure IXC–F). Hamartoma-like cells exhibited smooth muscle actin expression but also contained sarcomeric proteins which sometimes arranged into myofibrils (Figure 5J–K, Supplemental Figure IXG,I). Similar to clinical observations of naturally occurring hamartomas, we did not find any indication of a proliferative phenotype of hamartoma-like cells as we detected no cells staining positive for the proliferation marker Ki67 (Figure 5l, Supplemental Figure IXJ).

DISCUSSION

Preclinical development of potential cell therapies should be performed using clinically relevant cell production protocols and suitable animal models. This will involve production of cells in large batches followed by cryopreservation and direct delivery of cryopreserved cells after thaw as has been recently demonstrated[6] or processing them into an implantable product such as a cardiac patches or EHMs. As this will require GMP facilities which are not widely available, cardiac patches or EHMs will have to be robust enough to be transported to an application site. We have demonstrated that EHMs can be generated from human ESC-CMs in sufficient numbers for preclinical experiments and survive two to three days of shipment without impact on EHM function. Transport stability should facilitate the potential clinical translation of this approach.

We used two spinner flask differentiation batches and two monolayer differentiation batches to generate all the CMs and reporter line CMs required for this study. The cardiomyocyte yield varied from 70–95%, EHMs made from these batches showed small differences in cardiomyocyte content and contractile forces. In contrast to monolayer cultures where cells that died after thawing and plating are discarded with media changes, tissue engineered constructs retain cells which died during the formation. In this context, it is important to note that “plating” efficiency of cryopreserved CMs is generally similar (50–80%) in classical monolayer and EHM culture. Thus a high count for nuclear fragmentation of apoptotic cells in EHM leads to an overestimation of cell death due to 3D culture. Likewise, dead CMs do not stain positive for cardiac markers and can hence not be separated from non-CMs. These differences need to be considered when EHM (typical thickness 0.8–1 mm) are compared against thin tissue engineered constructs or single cell sheets with thicknesses <70 μm. Given the different techniques and shapes used to make cardiac tissues, comparing contractile forces on a force per cell basis may be a more suitable comparison. Our EHM loops generated 1.07±0.84 nN force/viable CM which is similar to previous reports[27, 28]. The microstructure of tissue engineered constructs is dependent on the geometry and production process. In line with previous publications, the EHMs exhibited CM alignment along the major strain axis and low expression levels of the gap junction protein connexin 43 as is anticipated for embryonic CMs[17, 27, 28].

While transport stability is an important parameter, long-term survival and functional integration are arguably the most important aims for regenerative cell therapies. Previous studies have primarily relied on histological assessments performed one month or earlier after implantation[8, 13, 14, 19, 29]. Although instructive, assessments of graft size and survival

kinetics are difficult to estimate histologically. BLI imaging of genetically modified reporter cell lines allows the non-invasive tracking of cell survival over time. Using our approach, we found that cell death was limited to the first two weeks following implantation with no significant cell loss afterwards up to 85 days. Cell survival/engraftment did not change after the second week following transplantation. This indicates that engrafted cells should survive for the entire lifespan of the animal. EHM implantation led to long term engraftment rates of 25% in some animals, exceeding previously reported engraftment rates of < 5% for single cell suspensions[10, 11]. The factors responsible for cell death observed during the first two weeks are difficult to parse out. It is likely that diffusion-limited supply of nutrients and oxygen is an important component, particularly since EHMs are not immediately perfused via a preformed vasculature. In contrast, EHMs are vascularized via an ingrowth of capillaries[15, 30]. Previous studies have indicated that including endothelial cells in tissue engineered constructs can lead to improved engraftment rates[29, 31]. However, it is difficult to attribute this better engraftment to faster revascularization since timescales for that have not been assessed. Moreover, the presence of endothelial cells or even preformed capillaries per se does not resolve the issue of lack of immediately communicating vasculature. A potential limitation of our approach is the use of a constituently active reporter ESC cell line where the expression of luciferase is not coupled to the expression of cardiac genes. Nonetheless, with a CM purity of approximately 90% following differentiation of the reporter line and grafts consisting almost exclusively of human CMs, it is very likely that the survival and engraftment estimates accurately track the behaviour of human CMs.

Composition and cellular phenotype of grafts are important considerations when assessing the ability of implanted structures to integrate into the host myocardium. One month after implantation, EHMs contained a host-derived vascular network similar to previous reports for cell injections[6] and patch transplantations[29, 32]. Although EHMs contained dead cells, CMs aligned in band-like structures, and fibroblasts *in vitro*, one month after implantation, grafts consisted of densely packed living human CMs that showed limited sarcomere alignment, similar to previous reports for cell injections[4] or patch transplantations[15]. The lack of fibroblasts in grafts indicates a preferential survival of human CMs since EHMs were made from cell batches containing up to 30% of fibroblasts. Grafts contained few macrophages, indicating that grafts had stabilized at this time point in concordance with our BLI data. Connexin 43 expression was low and poorly organized in these grafts, indicating the immature phenotype of these CMs, consistent with what - has been demonstrated previously[32, 33].

EHMs demonstrated good engraftment and survival by longitudinal BLI and post-mortem histology, we therefore decided to assess functional changes in the recipient hearts in a clinically relevant chronic rat MI model since there are already many available treatment options for acute MI. Standard of care treatment for acute MI in humans includes the use of antithrombotic drugs, anti-platelet therapies, and rapid reperfusion of the culprit vessel. These measures alleviate myocardial ischemia and reduce scar sizes. New developments such as drug eluting stents, modulation of inflammation, inhibition of apoptosis pathways, post conditioning, and blocking of mitochondrial transmembrane pore opening are currently under investigation[34]. In addition to these pharmacological approaches, adult stem cell

therapies are currently being tested as a potential treatment option for acute and sub-acute MI[7]. Although improvements in the treatment in acute MI have been made, a substantial number of patients will progress to heart failure. This patient population with chronic MI would benefit most from regenerative therapies that can reduce adverse remodelling and restore contractility.

In our study, we used a 1 hour I/R model which led to moderate rat heart infarct sizes (approx. 10% of LVM) and performed therapeutic interventions one month after MI. Cardiac MRI illustrated continued dilative remodelling in all groups, but significantly faster increases in end-systolic volumes were observed for the control group. EHM implantation significantly reduced the decline in ejection fraction compared to the control group. However, there were no significant differences between EHMs or irradiated EHMs which did not contain any viable human cells, indicating that the observed effect is not be mediated by living cells, but likely mechanical and/or immune cell related. Our data implies that despite high engraftment rates and stable long term survival of human ESC-CMs, recipient rat hearts did not show any functional improvements attributable to cell transplantation in this chronic MI model. While this may be surprising in light of previous published studies that found functional improvements, however those studies were primarily observations in acute and sub-acute models with cell delivery shortly after MI[4, 5, 19, 35, 36]. Paracrine factors may have a limited impact on chronic scar tissue, and mechanical contributions are unlikely from human CMs which cannot contract at the rate of the recipient rat heart (~400 bpm). A similar observation has previously been made for direct injection of human ESC-CMs into a chronic rat MI model which also failed to find functional improvements[37]. There is limited data available assessing functional improvements in rats following transplantation of tissue engineered constructs or cell sheets containing human CMs and none of them have used a chronic MI model[19]. It is also possible that longer observation periods are required to observe beneficial effects from human CM survival in chronic rodent MI models. We observed a high number of fibroblasts or myofibroblasts in irradiated EHMs, but we did not observe any changes in diastolic function for control or EHM groups. Any material or tissue engineered construct transplanted onto the heart might affect diastolic function. More detailed studies are needed to systematically address the risk of clinically relevant diastolic dysfunction associated with tissue engineered heart repair.

A xenogeneic cell transplantation model in rats can only give limited information on functional coupling of contractile human cardiomyocytes. Electrical coupling of human CMs with rat hearts has never been demonstrated likely due to inherent heart rate differences (60–120 bpm vs. 400 bpm). In contrast, electrical coupling of human CMs has been demonstrated in a guinea-pig model with heart rates of 200–250 bpm[38]. While electrical coupling is a prerequisite for mechanical force contribution from transplanted cells, the lack of immune deficient guinea-pig or larger animal models renders these models unsuitable for long-term engraftment, cell maturation, vascularisation, and tumor/teratoma risk assessment. Accordingly immunocompromised rat xenograft models are of high regulatory relevance (according to FDA and the Paul-Ehrlich-Institute). However, the lack of electrical integration reduces the utility of rodent models to assess arrhythmia risk which could be high due to the immature phenotype of CMs at the time of transplantation. A recent study observed substantial albeit non-life threatening arrhythmia after injection of 1×10^9

CMs into the myocardium of non-human primates[6]. Large animal studies will be required to assess the arrhythmia risk from EHM transplantation. In contrast to grafts at one month after implantation, grafts which had been implanted for more than three months showed a higher vascular density. Long-term engraftment also improved sarcomere structure and alignment as well as connexin 43 expression patterns. This was particularly evident for transplants that had been engrafted for 220 days, where connexin 43 expression exhibited a pattern typical for early postnatal stages in humans[39], which has not been reported for ESC-CMs thus far[5, 6, 37]. This data indicates that transplanted human CMs will mature in the host even in a xenogeneic setting. Prolonged survival of CMs exposed to cyclical stress and electrical stimulation is likely important for improved maturation. However, additional research will be required to assess if other factors present in the local environment play a role in this process as well.

While this is encouraging, we also noticed the appearance of foci of glycogen-rich cardiomyocytes in grafts that had been implanted for more than three month. These non-proliferating collections of cardiomyocytes expressed cardiac markers, but had overly abundant glycogen exhibiting a hamartoma-like phenotype[40, 41]. The exact histogenesis of these foci is not known, but reports in pediatric cardiac hamartomas have indicated that they may regress over time[42]. Interestingly, a hamartoma-like cardiomyocyte phenotype has not been described previously for ESC-CMs, which might be due to differences in the differentiation protocols, EHM manufacture, and or the longer engraftment period assessed in this study[4, 6, 29, 32, 37].

Potential safety implications of hamartoma-like cells will require further characterization, particularly the reversibility of this CM phenotype. No disconcerting evidence for other safety parameters was found: we did not observe any animal death during our studies, indicating that lethal arrhythmias did not occur, nor did we observe any tumors or teratomas in any of the animals used for this study.

In summary, this study demonstrates that implantation of EHMs made from human ESC-CMs leads to long-term engraftment of implanted cells in a chronic MI model. We observed progressive maturation of human grafts with sarcomere alignment after three month and enhanced connexin distribution supporting the notion that ESC-CMs can mature *in vivo* in a xenogeneic setting. Advancing tissue engineered heart repair into relevant large animal models will be a key step to demonstrate both safety and preliminary efficacy, in order to enable clinical translation.

Supplementary Material

Refer to Web version on PubMed Central for supplementary material.

Acknowledgments

We would like to thank Laura J. Pisani from the Stanford Small Animal Imaging Facility and Kitty Lee from the Cell Science Imaging Facility for their help with MRI and confocal imaging. We would also like to thank Andreas Schraut for his technical assistance.

SOURCES OF FUNDING

J.R. is supported by an Erwin Schrödinger fellowship from the Austrian Science Fund (FWF, J3314-B23). J.C.W. is supported by U01 HL099776, Leducq Foundation, AHA 13EIA14420025, CIRM RT3-07798, and CIRM TR3-05556 (JCW). E.N. is supported by AHA 11IRG5450017. U.R was supported by a German Research Foundation grant (DFG, RA 2179/1-1). W.H.Z. is supported by DZHK (German Center for Cardiovascular Research), German Federal Ministry for Science and Education (BMBF FKZ 13GW0007A), German Research Foundation (DFG SFB 1002 C04 and 937 A18), European Union FP7 CARE-MI, Leducq Foundation, and CIRM TR3-05556.

Nonstandard Abbreviations and Acronyms

BLI	bioluminescence imaging
CMs	cardiomyocytes
cTnT	cardiac Troponin T
EHM	engineered heart muscle
ESC-CMs	human embryonic stem cell derived cardiomyocytes
ESCs	embryonic stem cells
FACS	fluorescence activated cell sorting
Fluc-tdT	Firefly luciferase and tdTomato ESC reporter line
GMP	good manufacturing practice
hNA	human nuclear antigen
I/R	ischemia/reperfusion
iPSCs	induced pluripotent stem cells
LAD	left anterior descending
MI	myocardial infraction
MRI	magnetic resonance imaging
PSCs	pluripotent stem cells
SD	Sprague Dawley
TUNEL	terminal deoxynucleotidyl transferase (TdT) dUTP nick-end labelling

References

1. Laflamme MA, Murry CE. Heart regeneration. Nature. 2011; 473:326–35. [PubMed: 21593865]
2. Jessup M, Brozena S. Heart failure. N Engl J Med. 2003; 348:2007–18. [PubMed: 12748317]
3. Burridge PW, Keller G, Gold JD, Wu JC. Production of de novo cardiomyocytes: human pluripotent stem cell differentiation and direct reprogramming. Cell Stem Cell. 2012; 10:16–28. [PubMed: 22226352]
4. Laflamme MA, Chen KY, Naumova AV, Muskheli V, Fugate JA, Dupras SK, Reinecke H, Xu C, Hassanipour M, Police S, O'Sullivan C, Collins L, Chen Y, Minami E, Gill EA, Ueno S, Yuan C, Gold J, Murry CE. Cardiomyocytes derived from human embryonic stem cells in pro-survival factors enhance function of infarcted rat hearts. Nat Biotechnol. 2007; 25:1015–24. [PubMed: 17721512]
5. van Laake LW, Passier R, Monshouwer-Kloots J, Verkleij AJ, Lips DJ, Freund C, den Ouden K, Ward-van Oostwaard D, Korving J, Tertoolen LG, van Echteld CJ, Doevendans PA, Mummery CL. Human embryonic stem cell-derived cardiomyocytes survive and mature in the mouse heart and

transiently improve function after myocardial infarction. Stem Cell Res. 2007; 1:9–24. [PubMed: 19383383]

6. Chong JJ, Yang X, Don CW, Minami E, Liu YW, Weyers JJ, Mahoney WM, Van Biber B, Cook SM, Palpant NJ, Gantz JA, Fugate JA, Muskheli V, Gough GM, Vogel KW, Astley CA, Hotchkiss CE, Baldessari A, Pabon L, Reinecke H, Gill EA, Nelson V, Kiem HP, Laflamme MA, Murry CE. Human embryonic-stem-cell-derived cardiomyocytes regenerate non-human primate hearts. Nature. 2014; 510:273–7. [PubMed: 24776797]
7. Matsa E, Sallam K, Wu JC. Cardiac stem cell biology: glimpse of the past, present, and future. Circ Res. 2014; 114:21–7. [PubMed: 24385505]
8. Zimmermann WH, Melnychenko I, Wasmeier G, Didie M, Naito H, Nixdorff U, Hess A, Budinsky L, Brune K, Michaelis B, Dhein S, Schwoerer A, Ehmke H, Eschenhagen T. Engineered heart tissue grafts improve systolic and diastolic function in infarcted rat hearts. Nat Med. 2006; 12:452–8. [PubMed: 16582915]
9. Didie M, Christalla P, Rubart M, Muppala V, Doker S, Unsold B, El-Armouche A, Rau T, Eschenhagen T, Schwoerer AP, Ehmke H, Schumacher U, Fuchs S, Lange C, Becker A, Tao W, Scherschel JA, Soonpaa MH, Yang T, Lin Q, Zenke M, Han DW, Scholer HR, Rudolph C, Steinemann D, Schlegelberger B, Kattman S, Witty A, Keller G, Field LJ, Zimmermann WH. Parthenogenetic stem cells for tissue-engineered heart repair. J Clin Invest. 2013; 123:1285–98. [PubMed: 23434590]
10. van der Bogt KE, Sheikh AY, Schrepfer S, Hoyt G, Cao F, Ransohoff KJ, Swijnenburg RJ, Pearl J, Lee A, Fischbein M, Contag CH, Robbins RC, Wu JC. Comparison of different adult stem cell types for treatment of myocardial ischemia. Circulation. 2008; 118:S121–9. [PubMed: 18824743]
11. Li Z, Wilson KD, Smith B, Kraft DL, Jia F, Huang M, Xie X, Robbins RC, Gambhir SS, Weissman IL, Wu JC. Functional and transcriptional characterization of human embryonic stem cell-derived endothelial cells for treatment of myocardial infarction. PLoS One. 2009; 4:e8443. [PubMed: 20046878]
12. Ye L, Zimmermann WH, Garry DJ, Zhang J. Patching the heart: cardiac repair from within and outside. Circ Res. 2013; 113:922–32. [PubMed: 24030022]
13. Leontyev S, Schlegel F, Spath C, Schmiedel R, Nichtitz M, Boldt A, Rubsamen R, Salameh A, Kostelka M, Mohr FW, Dhein S. Transplantation of engineered heart tissue as a biological cardiac assist device for treatment of dilated cardiomyopathy. Eur J Heart Fail. 2013; 15:23–35. [PubMed: 23243122]
14. Miyahara Y, Nagaya N, Kataoka M, Yanagawa B, Tanaka K, Hao H, Ishino K, Ishida H, Shimizu T, Kangawa K, Sano S, Okano T, Kitamura S, Mori H. Monolayered mesenchymal stem cells repair scarred myocardium after myocardial infarction. Nat Med. 2006; 12:459–65. [PubMed: 16582917]
15. Tulloch NL, Muskheli V, Razumova MV, Korte FS, Regnier M, Hauch KD, Pabon L, Reinecke H, Murry CE. Growth of engineered human myocardium with mechanical loading and vascular coculture. Circ Res. 2011; 109:47–59. [PubMed: 21597009]
16. Stevens KR, Pabon L, Muskheli V, Murry CE. Scaffold-free human cardiac tissue patch created from embryonic stem cells. Tissue Eng Part A. 2009; 15:1211–22. [PubMed: 19063661]
17. Zhang D, Shadrin IY, Lam J, Xian HQ, Snodgrass HR, Bursac N. Tissue-engineered cardiac patch for advanced functional maturation of human ESC-derived cardiomyocytes. Biomaterials. 2013; 34:5813–20. [PubMed: 23642535]
18. Menasche P, Vanneaux V, Fabreguettes JR, Bel A, Tosca L, Garcia S, Bellamy V, Farouz Y, Pouly J, Damour O, Perier MC, Desnos M, Hagege A, Agbulut O, Bruneval P, Tachdjian G, Trouvin JH, Larghero J. Towards a clinical use of human embryonic stem cell-derived cardiac progenitors: a translational experience. Eur Heart J. 2014
19. Masumoto H, Ikuno T, Takeda M, Fukushima H, Marui A, Katayama S, Shimizu T, Ikeda T, Okano T, Sakata R, Yamashita JK. Human iPS cell-engineered cardiac tissue sheets with cardiomyocytes and vascular cells for cardiac regeneration. Sci Rep. 2014; 4:6716. [PubMed: 25336194]
20. Chen VC, Couture SM, Ye J, Lin Z, Hua G, Huang HI, Wu J, Hsu D, Carpenter MK, Couture LA. Scalable GMP compliant suspension culture system for human ES cells. Stem Cell Res. 2012; 8:388–402. [PubMed: 22459095]

21. Tiburcy M, Meyer T, Soong PL, Zimmermann WH. Collagen-based engineered heart muscle. Methods Mol Biol. 2014; 1181:167–76. [PubMed: 25070336]
22. Zimmermann WH, Fink C, Kralisch D, Remmers U, Weil J, Eschenhagen T. Three-dimensional engineered heart tissue from neonatal rat cardiac myocytes. Biotechnol Bioeng. 2000; 68:106–14. [PubMed: 10699878]
23. Cao F, Lin S, Xie X, Ray P, Patel M, Zhang X, Drukker M, Dylla SJ, Connolly AJ, Chen X, Weissman IL, Gambhir SS, Wu JC. In vivo visualization of embryonic stem cell survival, proliferation, and migration after cardiac delivery. Circulation. 2006; 113:1005–14. [PubMed: 16476845]
24. Huber BC, Ransohoff JD, Ransohoff KJ, Riegler J, Ebert A, Kodo K, Gong Y, Sanchez-Freire V, Dey D, Kooreman NG, Diecke S, Zhang WY, Odegaard J, Hu S, Gold JD, Robbins RC, Wu JC. Costimulation-adhesion blockade is superior to cyclosporine A and prednisone immunosuppressive therapy for preventing rejection of differentiated human embryonic stem cells following transplantation. Stem cells. 2013; 31:2354–63. [PubMed: 24038578]
25. Riegler J, Cheung KK, Man YF, Cleary JO, Price AN, Lythgoe MF. Comparison of segmentation methods for MRI measurement of cardiac function in rats. J Magn Reson Imaging. 2010; 32:869–77. [PubMed: 20882617]
26. Du J, Liu J, Feng HZ, Hossain MM, Gobara N, Zhang C, Li Y, Jean-Charles PY, Jin JP, Huang XP. Impaired relaxation is the main manifestation in transgenic mice expressing a restrictive cardiomyopathy mutation, R193H, in cardiac TnI. Am J Physiol Heart Circ Physiol. 2008; 294:H2604–13. [PubMed: 18408133]
27. Turnbull IC, Karakikes I, Serrao GW, Backeris P, Lee JJ, Xie C, Senyei G, Gordon RE, Li RA, Akar FG, Hajjar RJ, Hulot JS, Costa KD. Advancing functional engineered cardiac tissues toward a preclinical model of human myocardium. FASEB J. 2014; 28:644–54. [PubMed: 24174427]
28. Kensah G, Roa Lara A, Dahlmann J, Zweigerdt R, Schwanke K, Hegermann J, Skvorc D, Gawol A, Azizian A, Wagner S, Maier LS, Krause A, Drager G, Ochs M, Haverich A, Gruh I, Martin U. Murine and human pluripotent stem cell-derived cardiac bodies form contractile myocardial tissue in vitro. Eur Heart J. 2013; 34:1134–46. [PubMed: 23103664]
29. Stevens KR, Kreutziger KL, Dupras SK, Korte FS, Regnier M, Muskheli V, Nourse MB, Bendixen K, Reinecke H, Murry CE. Physiological function and transplantation of scaffold-free and vascularized human cardiac muscle tissue. Proc Natl Acad Sci U S A. 2009; 106:16568–73. [PubMed: 19805339]
30. Riegler J, Gillich A, Shen Q, Gold JD, Wu JC. Cardiac tissue slice transplantation as a model to assess tissue-engineered graft thickness, survival, and function. Circulation. 2014; 130:S77–86. [PubMed: 25200059]
31. Sekine H, Shimizu T, Hobo K, Sekiya S, Yang J, Yamato M, Kurosawa H, Kobayashi E, Okano T. Endothelial cell coculture within tissue-engineered cardiomyocyte sheets enhances neovascularization and improves cardiac function of ischemic hearts. Circulation. 2008; 118:S145–52. [PubMed: 18824746]
32. Caspi O, Lesman A, Basevitch Y, Gepstein A, Arbel G, Habib IH, Gepstein L, Levenberg S. Tissue engineering of vascularized cardiac muscle from human embryonic stem cells. Circ Res. 2007; 100:263–72. [PubMed: 17218605]
33. Feinberg AW, Ripplinger CM, van der Meer P, Sheehy SP, Domian I, Chien KR, Parker KK. Functional differences in engineered myocardium from embryonic stem cell-derived versus neonatal cardiomyocytes. Stem Cell Reports. 2013; 1:387–96. [PubMed: 24286027]
34. Windecker S, Bax JJ, Myat A, Stone GW, Marber MS. Future treatment strategies in ST-segment elevation myocardial infarction. Lancet. 2013; 382:644–57. [PubMed: 23953388]
35. Caspi O, Huber I, Kehat I, Habib M, Arbel G, Gepstein A, Yankelson L, Aronson D, Beyar R, Gepstein L. Transplantation of human embryonic stem cell-derived cardiomyocytes improves myocardial performance in infarcted rat hearts. Journal of the American College of Cardiology. 2007; 50:1884–93. [PubMed: 17980256]
36. Leor J, Gerecht S, Cohen S, Miller L, Holbova R, Ziskind A, Shachar M, Feinberg MS, Guetta E, Itskovitz-Eldor J. Human embryonic stem cell transplantation to repair the infarcted myocardium. Heart. 2007; 93:1278–84. [PubMed: 17566061]

37. Fernandes S, Naumova AV, Zhu WZ, Laflamme MA, Gold J, Murry CE. Human embryonic stem cell-derived cardiomyocytes engraft but do not alter cardiac remodeling after chronic infarction in rats. J Mol Cell Cardiol. 2010; 49:941–9. [PubMed: 20854826]

38. Shiba Y, Fernandes S, Zhu WZ, Filice D, Muskheli V, Kim J, Palpant NJ, Gantz J, Moyes KW, Reinecke H, Van Biber B, Dardas T, Mignone JL, Izawa A, Hanna R, Viswanathan M, Gold JD, Kotlikoff MI, Sarvazyan N, Kay MW, Murry CE, Laflamme MA. Human ES-cell-derived cardiomyocytes electrically couple and suppress arrhythmias in injured hearts. Nature. 2012; 489:322–5. [PubMed: 22864415]

39. Vreeker A, van Stuijvenberg L, Hund TJ, Mohler PJ, Nikkels PG, van Veen TA. Assembly of the cardiac intercalated disk during pre- and postnatal development of the human heart. PLoS One. 2014; 9:e94722. [PubMed: 24733085]

40. Padalino MA, Vida VL, Bhattarai A, Reffo E, Milanesi O, Thiene G, Stellin G, Basso C. Giant intramural left ventricular rhabdomyoma in a newborn. Circulation. 2011; 124:2275–7. [PubMed: 22083149]

41. Radi ZA, Metz A. Canine cardiac rhabdomyoma. Toxicol Pathol. 2009; 37:348–50. [PubMed: 19380844]

42. Farooki ZQ, Ross RD, Paridon SM, Humes RA, Karpawich PP, Pinsky WW. Spontaneous regression of cardiac rhabdomyoma. Am J Cardiol. 1991; 67:897–9. [PubMed: 2011993]

Novelty and Significance

What Is Known?

- Cardiomyocyte loss after myocardial infarction can lead to deleterious remodelling of the heart culminating in heart failure.
- Transplantation of human embryonic stem cell-derived cardiomyocytes (ESC-CMs) shortly after experimentally induced myocardial infarction improves cardiac function in animal models.
- Survival of ESC-CMs following transplantation is low, potentially limiting the efficacy of this approach.

What New Information Does This Article Contribute?

- Transplantation of ESC-CMs as macroscopic tissue engineered structures leads to high cell engraftment rates and stable long-term survival.
- ESC-CM engraftment did not correlate with functional improvements in a rodent model where cells are transplanted one month after myocardial infarction.
- ESC-CM transplantation was safe as no tumors or teratomas where detected during long-term follow up.

Cardiac regeneration requires the replacement of cardiomyocytes lost during periods of oxygen undersupply such as myocardial infarction. This may be achieved by delivering ESC-CMs. However, survival of transplanted cells in the heart is very low, limiting the feasibility of this approach. In this study, we provide evidence that tissue engineering approaches can improve cell retention and lead to long-term engraftment and survival of transplanted cells. Furthermore, progressive structural maturation of transplanted human cardiomyocytes was observed. Although engraftment is a prerequisite for functional benefits from active force generation by transplanted cells, we did not observe such benefits in a chronic myocardial infarction model. This indicates that functional benefits from human cardiomyocytes may not be accurately estimated in rodent myocardial infarction models. However, rodent models are suitable to assess long-term cell survival as well as tumor or teratoma risk which are difficult to assess in larger animals where immunocompromised strains do not exist. Our study shows that transplantation of ESC-CMs did not lead tumor to or teratoma formation which are the primary safety concerns for therapies using cells derived from ESCs. These results encourage further translational research in large animal models to estimate the functional benefits from such a therapy.

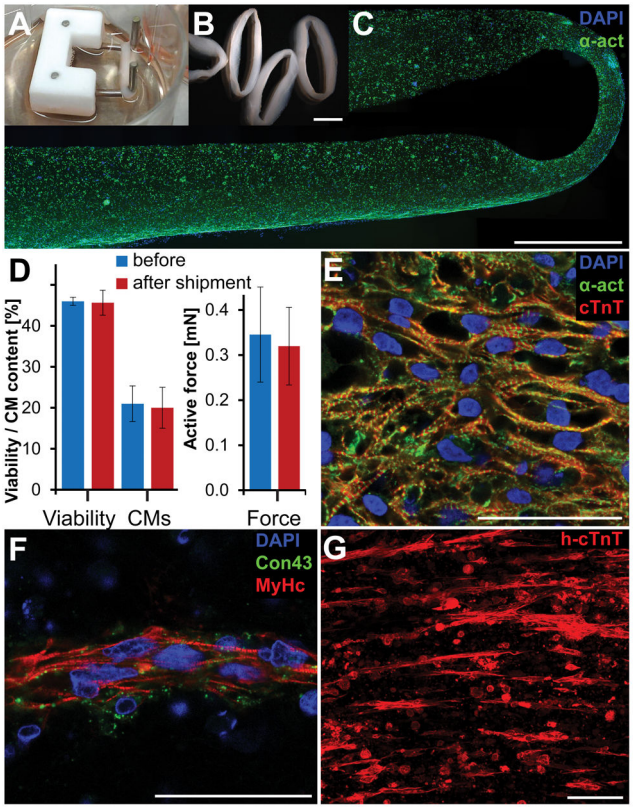

Figure 1. Human engineered heart muscle (EHM) show cardiomyocyte alignment, robustness in viability and force generation following two days of shipment

(A,B) Photographs of EHM on individual stretchers for mechanical maturation and on a plate prior to force testing. (C) Fluorescence microscopy image of an EHM illustrating the distribution of cardiomyocytes (alpha actinin, α-act) across its cross-section with slightly higher concentration along the outer boundaries. (D) Two days of shipment did not change cell viability (n=3, P=0.83), cardiomyocyte content (n=3, P=0.86), or active force generation (n=3, P=0.87). (E) Cardiac-like tissue organization of cardiomyocytes (human cardiac troponin T, cTnT) was found in some areas of EHMs particular towards the outer boundaries. (F) Most of the EHM cross sections showed cardiomyocyte (β myosin heavy chain, MyHc) alignment in band-like structures along the principle strain axis with low levels of connexin 43 (Con43) expression. (G) Band-like cell arrangement is further illustrated by a maximum intensity projection of a 250 μm thick imaging volume from the center of an EHM loop. Scale bars B: 5 mm; C: 1 mm; E,F: 50 μm; G: 100 μm.

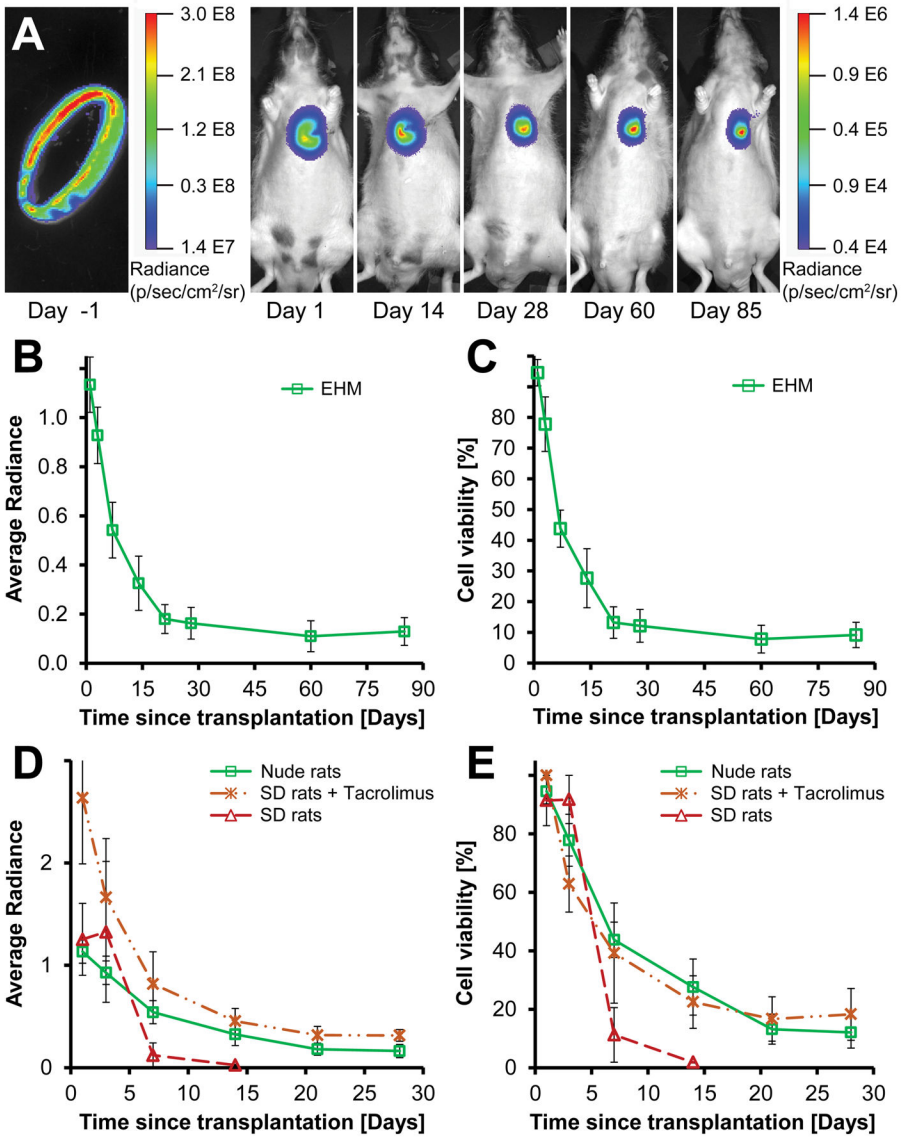

Figure 2. Human EHMs show long-term engraftment and survival

(A) Representative bioluminescence images of a single EHM loop *ex vivo* (left) and post-implantation up to 85 days (right). (B,C) EHMs showed no significant decline in viability between day 14 and 85 (n=6, P=0.33). (D) Implantation of EHM onto immunocompetent rat hearts (Sprague Dawley, SD) led to almost complete signal loss within 7 days (dashed red line, n=2). However, when Tacrolimus was administered twice daily (7.5 mg/kg/day), the BLI signal was comparable to that seen in nude rats, indicating that effective immune suppression was achieved. (E) Effective immune suppression in SD rats enabled graft survival comparable to nude rats (SD+Tac n=5 vs. nude n=6; P=0.88). Average radiance expressed as 10^6 photons/second/cm^2/steradian.

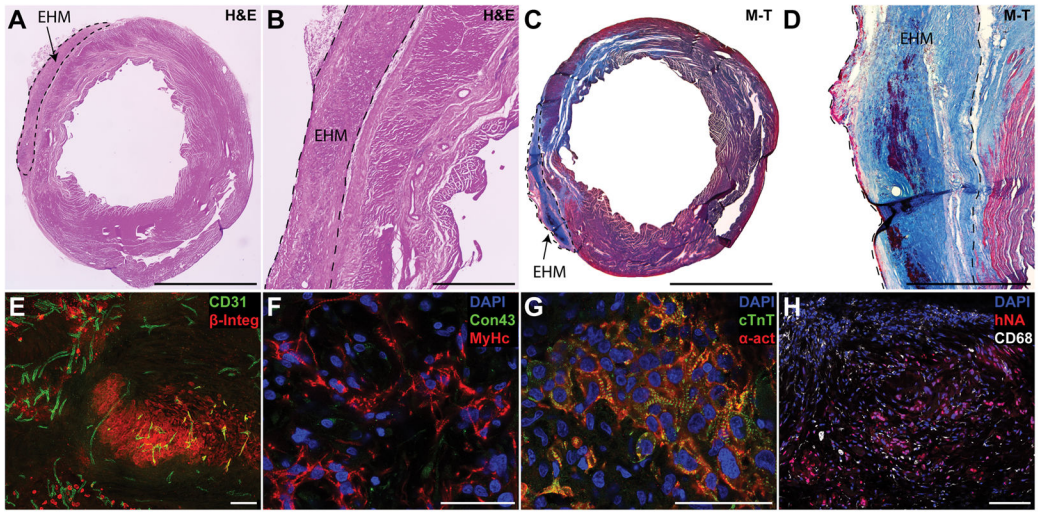

Figure 3. Sizable grafts of human cardiomyocytes could be found one month after EHM implantation

(A–D) One month after implantation EHM, grafts were found covering the scar area or border zone on H&E or Masson's trichrome (M–T) sections. EHMs were typically separated from the host by a small layer of fibrotic tissue. (E) Grafts staining positive for human beta integrin 1 (β-Integ) could be found for all EHM hearts assessed. Grafts were perfused by host vessels (CD31) that grew into the graft (maximum intensity projection of a 30 μm section). (F) Grafts consisted primarily of human CMs staining positive for beta myosin heavy chain (MyHc), but there were few cell junctions that stained positive for connexin 43 (Con43). (G) While clearly striated sarcomeres could be found (cardiac troponin T, cTnT; alpha sarcomeric actin, α-act) there were few signs of myofibril alignment. (H) EHMs showed few infiltrating macrophages (CD68) indicating stable grafts. Scale bars A,C: 5 mm; B,D: 1 mm; E,H: 100 μm; F,G: 50 μm.

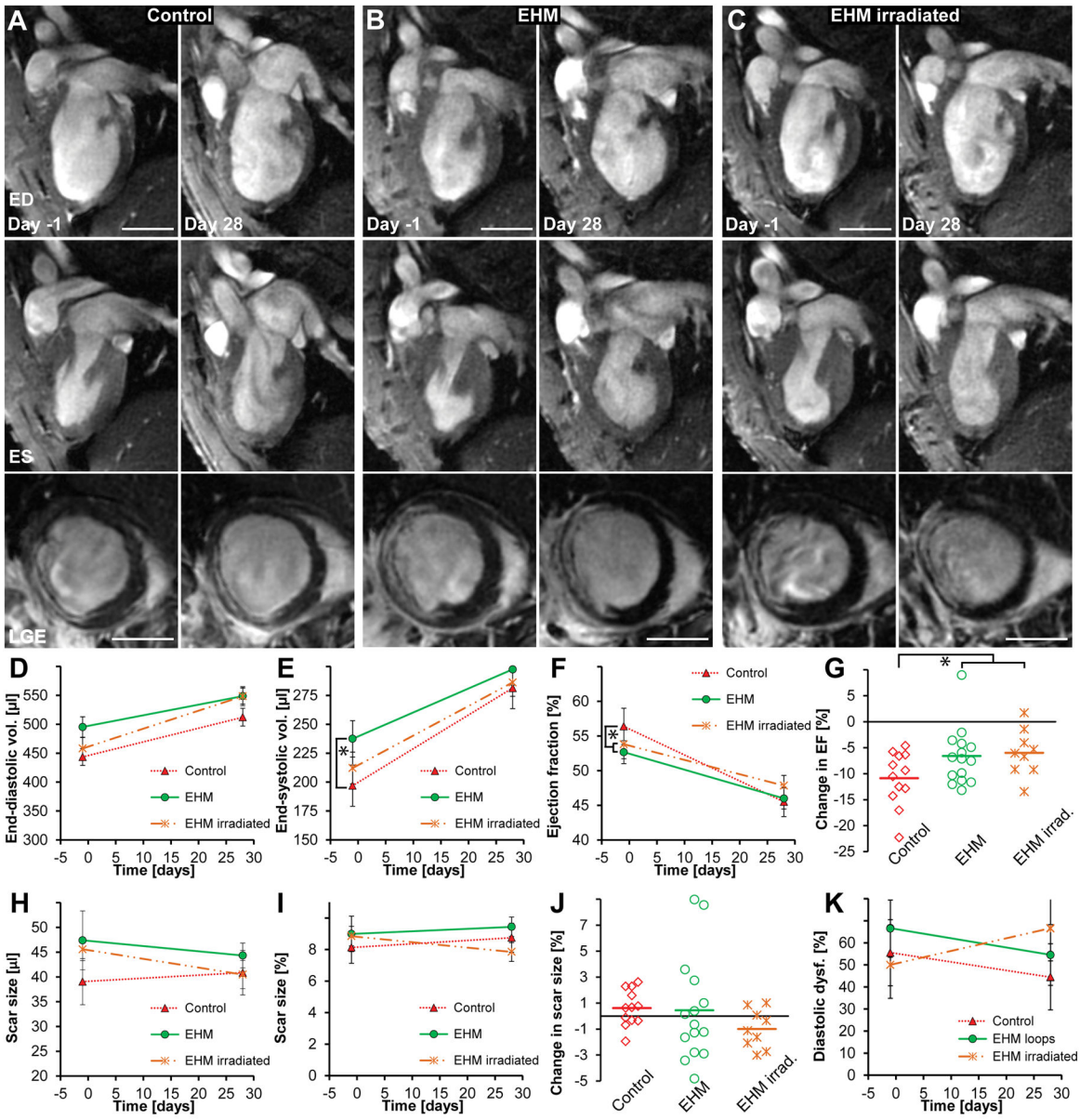

Figure 4. EHM implantation reduces dilative remodelling but this effect is not due to human CM engraftment

(A–C) The top row shows representative 2-chamber long-axis views at end-diastole (ED) one day prior to and 28 days after EHM implantation or sham surgery (control group). The middle row shows the same hearts at end-systole (ES) while the bottom row shows corresponding late gadolinium enhancement images (LGE) at mid-ventricular level. (D,E) End-diastolic volumes increased in all groups but were not significantly different (P=0.35). End-systolic volumes also increased in all groups, but the control group mas most pronounced compared to all other groups (control n=12 vs. EHM n=14; P=0.05). (F,G) Ejection fractions declined in all groups. The control group showed the highest relative decline compared to EHM implantation groups (P=0.03); however, there was no difference between EHMs or irradiated EHMs that did not contain viable CMs (P=0.19), indicating that

beneficial effects on remodelling may not be directly mediated by grafted cells. (H,I,J) No significant difference was observed for changes in scar size over time (P=0.32). (K) There was a trend toward increase in diastolic dysfunction (E′/A′ <1) for hearts receiving irradiated EHM loops while a small decline was observed for the other groups; however, this did not reach statistical significance (P=0.12). Scale bars A–C: 5 mm.

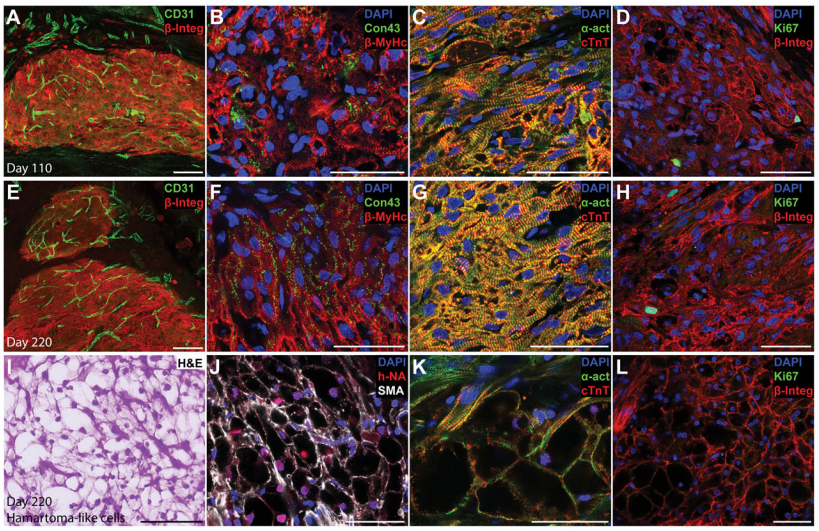

Figure 5. Long-term grafts showed high blood vessel density, progressive cardiomyocyte alignment and connexin 43 expression

(A,E) A high blood vessel density (CD31, maximum intensity projection of a 30 μm section) was found in human grafts (human beta 1 integrin, β-Integ) at 110 and 220 days after implantation. (B,F) Connexin (connexion 43, Con43) expression could be detected in 110 day old grafts (B), but grafts which were implanted for 220 days showed a more mature expression pattern with connexin localised at cell interfaces (F). Sarcomere alignment also increased with time in human CMs (beta myosin heavy chain, β-MyHc). (C–D) Long-term engraftment led to better sarcomere alignment and more mature sarcomeres (alpha sarcomeric actinin, α-act; cardiac troponin T, cTnT) spanning the entire width of CMs. (D,H) Only a small number of human cells showed signs of an active cell cycle (Ki67) after 110 or 220 days of engraftment. (I) Interestingly, the 220-day-old grafts contained small foci where CMs showed a glycogen-rich, hamartoma-like phenotype (H&E). (J,K) These hamartoma-like cells were of human origin (human nuclear antigen, hNA) and stained positive for smooth muscle actin (SMA) as well as cardiac markers (α-act, cTnT), with some showing organised sarcomeres. (L) None of the hamartoma-like cardiomyocytes was in an active state of the cell cycle (Ki67, negative). Scale bars A,E,I: 100 μm; B–D, F–H, J–L: 50 μm.